Peak-to-Average Power Ratio Suppression using Companding schemes in OFDM Systems

Abdulwahid Mohammed[1], Mohamed Shehata[1], Hassan Mostafa[1,2], Amin Nassar[1]
[1]Electronics and Communication Engineering Department, Cairo University, Giza 12613, Egypt.
[2]Nanotechnology and Nanoelectronics program at Zewail City for Science and Technology, Giza 12588, Egypt

***Abstract*—The reduction of the high signal peak-to-average-power-ratio (PAPR) in orthogonal frequency division multiplexing (OFDM) systems limits the clipping-induced non-linear harmonic distortions caused by power amplifiers. In this paper, the characteristics of the circuits implemented in sub-threshold CMOS are employed to perform companding-based PAPR reduction for OFDM signals. Simulation results confirm that the tanh-companding amplifiers are capable of reducing the PAPR of OFDM signals through the careful control of their design parameters.**

***Index Terms*—Companding, orthogonal frequency division multiplexing (OFDM), peak to average power ratio (PAPR).**

I. INTRODUCTION

Orthogonal frequency division multiplexing (OFDM) is one of the spectrally efficient multi-carrier (MC) transmission techniques. In OFDM-based systems, a large number of independent narrowband signals are simultaneously transmitted over a set of orthogonal carriers whose frequencies are closely spaced in the frequency domain. The high spectral utilization offered by OFDM transmission is one of the reasons behind its adoption as the core system of many air-interface standards. These standards include, but not limited to, worldwide interoperability for microwave access (WiMAX), terrestrial digital video broadcasting (DVB-T) and the IEEE 802.11a standard for wireless local area networks (WLANs). Moreover, due to its robustness against multipath propagation effects in high-mobility environments, OFDM has been widely adopted for 4G communications. Moreover, the immunity of OFDM to impulsive noise has also recommended its use in wire-line applications, such as power line communications (PLC) and digital subscriber lines (DSL) [1].

As an MC transmission technique, the orthogonal sub-carriers in OFDM-based systems might sum up instantaneously and abruptly to the same phase. This constructive phase addition leads to a large increase in the instantaneous OFDM signal power beyond the saturation limits of the power amplifier (PA) that usually precede a TX antenna. The value of the observed instantaneous power might reach up to several orders of magnitude of the average OFDM signal power, leading to clipping induced non-linearities. These clipping non-linearities induce irrecoverable out-of-band harmonic distortions [2], [3]. Consequently, a PA with a wide dynamic input range is often desired to ensure its operation in the linear regime [4]. Unfortunately, PAs with a large input dynamic range are not efficient in terms of their power conversion efficiency and/or the required bias conditions [5], [6]. Alternatively, peak-to-average-power-ratio (PAPR) reduction techniques are often applied to the OFDM signal before being forwarded to a PA. Companding the dynamic range of OFDM signals is one of the most popular PAPR reduction techniques due to its low implementation complexity and bandwidth requirements [7], [8]. Numerous techniques have been reported to reduce the PAPR of OFDM signals using non-linear input/output (I/O) characteristics (e.g., [9]–[11]).

In this work, the application of the non-linear I/O characteristics of practical amplifier designs as companding techniques in OFDM-based systems is proposed. Four different amplifier topologies, based on sub-threshold CMOS-based differential pairs [9], are recommended for this purpose. The I/O characteristics of the considered designs are scaled versions of the hyperbolic tangent (tanh) function. Throughout this work, the I/O characteristic relationships of the four considered designs are matched to that of the non-linear error function (NERF), which is one of the most commonly used companding techniques in OFDM-based systems. Simulation results show that the PAPR reduction performance of tanh-based companding is comparable to that of the NERF function, provided that the I/O characteristics of the sub-threshold CMOS-based differential pairs are carefully controlled. The rest of this paper is organized as follows. Section II overviews the general mathematical frame- work of OFDM-based systems. In Section III, a comprehensive definition of the PAPR is introduced whether or not a companding technique is applied. Moreover, a number of I/O characteristic relationship of the NERF companding function is over-viewed. The I/O characteristics of the four practical sub-threshold CMOS-based designs are also introduced. Section IV presents numerical simulation results that validate the proposal of using the design in [9] for companding-based PAPR reduction in OFDM communications.

II. OFDM-BASED SYSTEMS: MODEL OVERVIEW

Fig. 1 shows a typical block diagram of an OFDM transceiver chain that utilizes companding/de-companding technique to reduce the PAPR. The entire system is driven by an information source that emits a stream of independent and

978-1-5386-7392-8/18/$31.00 ©2018 IEEE

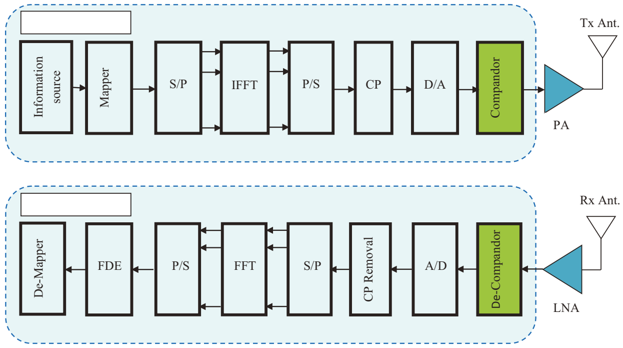

Fig. (1) Block diagram representation of a typical OFDM transceiver chain that employs companding/de-companding.

identically distributed (i.i.d) binary valued random variables (RVs) to a quadrature phase shift keying (QPSK) constellation mapper at a rate of R_b bps. At the output of the QPSK mapper, each N symbols are forwarded to a $1 \times N$ serial to parallel (S/P) converter at a rate of $R_s = R_b/2$ Sps. The S/P splits the input symbol stream into N parallel streams of R_s/N Sps rate each. The resulting N signals are applied to the N input ports of an inverse discrete Fourier transform (IDFT) processor before being converted to a corresponding N time domain parallel streams. A parallel-to-serial (P/S) converter is applied to the resulting time domain symbols, denoted by $\tilde{s}_n$ such that its output is expressed as follows [13]:

$$\tilde{s}_n = \sum_{k=0}^{N-1} \tilde{S}_k \exp(-j2\pi nk/N); 0 \leq n \leq N-1. \tag{1}$$

The complex time series in (1) constitute the useful information part of an OFDM symbol. The redundancy of this discrete-time sequence is increased by inserting the last N_{CP} of its samples as a cyclic prefix (CP). An analog form of (1) is obtained by applying a digital-to-analog (D/A) smoothing filter whose output is denoted by $\tilde{x}(t)$. At the transmitter front-end, the OFDM signal power is boosted by a PA before being emitted to the wireless channel via a TX antenna. To avoid the clipping-induced non-linearities introduced by the PA, a companding operator, denoted by $f(x)$, is independently applied to the real and the imaginary parts of $\tilde{x}(t)$ as follows:

$$\tilde{x}_{comp}(t) = f\left(\Re e\{\tilde{x}(t)\}\right) + jf\left(\Im e\{\tilde{x}(t)\}\right). \tag{2}$$

At the receiver front-end, the received signal, denoted by $\tilde{r}(t)$ is obtained by convolving (2) with the channel impulse response (CIR) $\tilde{h}(t)$, and is corrupted by a zero mean additive white Gaussian noise (AWGN) random process, denoted by $\mu(t)$. The CIR is given by $\tilde{h}(t) = \sum_{l=0}^{L-1} \tilde{c}\delta(t-\tau_l)$, where $\tilde{c}, \tau_l$ and L are given by the power-delay profile (PDP) of the channel. A de-companding operator, given by $f^{-1}(x)$, is applied to the received signal. The de-compandor output is sampled at a rate of f_s Sps by an analog-to-digital (D/A) converter and the CP redundancy is removed from the resulting time domain sequence. Assuming a perfect TX-RX synchronization, the N samples length time domain OFDM symbol is converted back to its frequency domain dual, denoted by $\tilde{Y}_k$, by using a S/P converter, a discrete Fourier transform processor and a P/S converter. This is expressed mathematically as follows:

$$\tilde{Y}_k = \tilde{H}_k \tilde{S}_k + \tilde{\nu}_n; 0 \leq k \leq N-1, \tag{3}$$

where $\tilde{H}_k = \frac{1}{\sqrt{N}} \sum_{k=0}^{N-1} \tilde{h}_n \exp(j2\pi nk/N)$ is the discrete frequency domain CIR, $\tilde{h}_n = \tilde{h}(t = n/f_s)$ is the time sampled CIR, $\tilde{\nu}_n = \frac{1}{\sqrt{N}} \sum_{k=0}^{N-1} \tilde{\mu}_n \exp(j2\pi nk/N), \tilde{\mu}_n = \tilde{\mu}(t = n/f_s)$ is the time sampled AWGN random process. The fading effects experienced by the OFDM signal over the wireless channel are compensated by applying a single tap zero forcing-frequency domain equalizer (ZF-FDE) to (3). The resulting equalized frequency domain symbols are then QPSK de-mapped into a binary data stream and the Bit Error Rate (BER) performance is given by $P_b = \frac{1}{2} \Pr\left\{\tilde{Y}_k \neq \tilde{S}_k\right\}$.

III. COMPANDING THE PEAK TO AVERAGE POWER RATIO

The PAPR of an arbitrary signal $x(t)$ is defined as the ratio of its peak power to its average power. Applying this definition to the transmitted OFDM signal in (2), a PAPR operator is expressed mathematically as [14]:

$$\mathbf{PAPR}\{f(x(t))\} = \frac{\max\{|f(x(t))|^2\}}{\mathbf{E}\{f(|x(t)|^2)\}}; -\infty \leq t \leq \infty. \tag{4}$$

Where, $\mathbf{E}\{.\}$ is the expectation operator, $f(.)$ is the companding operator, and $\max\{|x(t)|^2\}$ and $\mathbf{E}\{|x(t)|^2\}$ are the peak OFDM signal power and its average power, respectively. Clearly, the purpose of the companding operator is to increase the average value of the OFDM signal power and/or to decrease its peak instantaneous value.

A. Non-linear Error Function Companding

As its name implies, the non-linear error function (NERF) companding is based on the familiar Gaussian error function, and is expressed as [15]:

$$f(x) = sgn(x)k^{\gamma}\left[erf(\frac{|x|}{\sqrt{2}\sigma})\right]^{\gamma}, \tag{5}$$

where $k, \sigma \in \mathbf{R}^{+}$ are scaling constants that define the dynamic range of the input and the output signals, respectively, sgn(.) is the conventional signum function, defined as sgn(x) = 1; $x \geq 0$, sgn(x)= -1; $x < 0$ and $erf(z)$ is the conventional Gaussian error function, which is given by

$$erf(z) = \frac{2}{\sqrt{\pi}} \int_{0}^{z} \exp\left(-t^2\right) dt. \tag{6}$$

It should be noted that σ is the statistical standard deviation of $|x|$. In other words, the characteristics of the NERF companding function should be adaptively adjusted to the dynamic range of the input signal. Moreover, k, σ and γ are not independent. According to [15], $\gamma = 1$ and power conservative companding is assumed (i.e., $\mathbf{E}\{|f(x)|^2\} = \mathbf{E}\{|x|^2\}$). This yields $k = \sqrt{3}\sigma$. Alternatively, another form of NERF companding is obtained by setting $\gamma = 1/2$ [15]. Accordingly, the power conservative companding assumption yields $k = 2\sigma$.

B. The Equations of Designed Circuits for Differential Pair

In [12], differential tanh-companding is achieved using one of four possible MOSFET-based differential pair designs. For simplicity, the I/O characteristics of these four designs are reformulated as follows:

$$f_1(x) = \alpha \tanh\Big(\zeta x\Big), \tag{7}$$

$$f_2(x) = \beta \tanh\big(\zeta x + \frac{1}{2} ln(m)\big) + \beta \tanh\big(\zeta x - \frac{1}{2} ln(m)\big), \\ - 2\beta \tanh(\zeta x) + \alpha \tanh(\zeta x) \tag{8}$$

$$f_3(x) = \beta \tanh\big(\zeta x + \frac{1}{2} ln(m)\big) + \beta \tanh\big(\zeta x - \frac{1}{2} ln(m)\big), \tag{9}$$

$$f_4(x) = \alpha \tanh\left(\zeta x - \tanh^{-1}\left[\frac{\tanh\big(\zeta x\big)}{2m+1}\right]\right), \tag{10}$$

where, (7)-(10) correspond to the four designs considered in [12]. In each of the afore-mentioned designs, the values of the parameters α, β, ζ and m in (7)-(10) are matched to the values of k, σ and γ of the NERF companding characteristics in (5).

IV. SIMULATION RESULTS AND ANALYSIS

This section presents numerical simulation results for the OFDM system using the companding/de-companding techniques discussed in Section III, with the PAPR and the BER as the performance metrics of interest. The numerical values of the simulation parameters are as follows: A symbol rate of R_s = 9.6 kSps is assumed. Accordingly, the sampling frequency and the sub-carrier frequency spacing are $f_s = R_s$ and $\Delta f = f_s/N$ = 150 Hz, respectively. The BER is calculated using Monte-Carlo simulations by averaging a number of 1000 OFDM symbols. The size of the FFT/IFFT matrix is N = 64, whereas N_{CP} is set to 16 samples. Throughout simulations, it is assumed that $0 \leq |x| \leq 1, \gamma = 1, \sigma = 0.5817$ and $k = 1.0075$. Table (I) shows the different values of the tanh-companding amplifier parameters in (7)-(10) that match those of the NERF companding function. Moreover, a six paths Rayleigh fading channel model is assumed. Table (II) shows the power delay profile (PDP) of the adopted channel model [16].

TABLE (I) Design parameters of Eq (7-10)

	Design 1	Design 2	Design 3	Design 4
α	1	1	1	1
ζ	1.27	1.27	1.27	1.27
β	1	1	-	-
m	-	1.1972	0.04	19.5

The simulation starts by matching the design parameters in (7)-(10) to those of the NERF characteristics. The optimal parameter set for each design is listed in Table (II). Fig.(2) depicts the resulting matched characteristics.

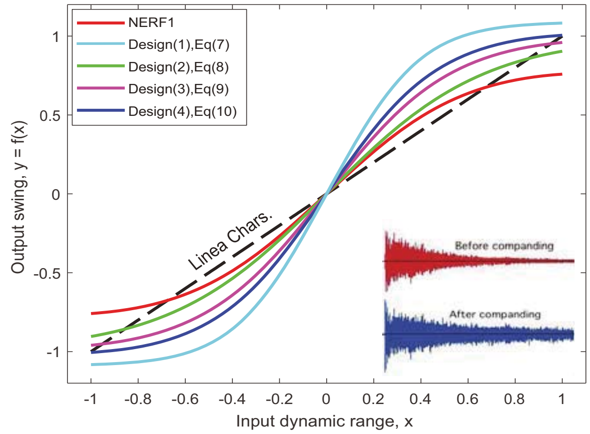

(a)

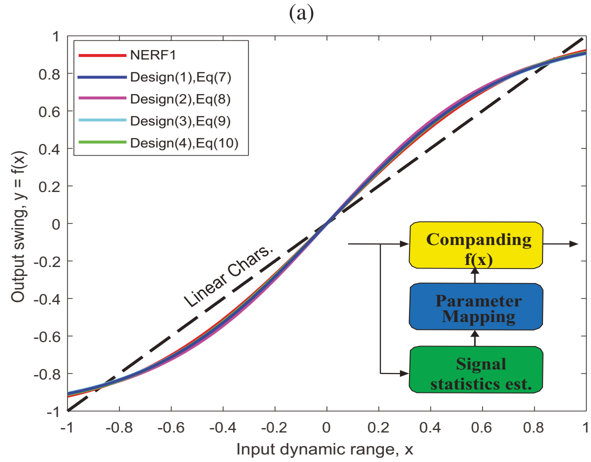

(b)

Fig. (2) NERF versus tanh-companding characteristics with (a): un-matched and (b): matched characteristics.

TABLE (II) Channel Power-Delay profile

Tap number	1	2	3	4	5	6
Power (dB)	-3	0	-2	-6	-8	-10
Delay (μs)	0	0.2	0.5	1.6	2.3	5

Figs. 3 (a) and (b) demonstrate the performance of the NERF companding in (5) as compared to I/O characteristics in (7)-(10). Fig. 3 (a) shows the complementary cumulative distribution function (CCDF) versus the PAPR for the considered companding techniques, whereas Fig. 3 (b) plots the BER performance versus the signal to noise ratio (SNR) for the same techniques in Fig. 3 (a). It is clear from Fig. 3 (a) that, NERF-based companding introduces a virtual gain of about 2 dB to an un-companded OFDM signal at a CCDF value as low as 10^{-3}. Moreover, a differential tanh-companding amplifier whose I/O characteristics are well-matched to the NERF function shows a very CCDF versus PAPR performance. The sub-figure in Fig. 3 (a) illustrates the negligible differences among the performances of the four amplifier designs.

Moreover, a reduction of about 1.89 dB (from 10.35 dB to 8.46 dB) in the PAPR of the OFDM signal is observed at a CCDF value of 10^{-3}. However, this improvement is accompanied by a slight deterioration in the BER performance, which increases with increasing the SNR as clear from Fig. (3a). Furthermore, a power penalty of no more than 1 dB is required for a companded OFDM system to achieve the same forward error correction (FEC) BER limit of 10^{-3} that is achieved by its un-companded counterpart. Applying the recommended approach (NERF companding technique) to MIMO systems will be investigated in future works.

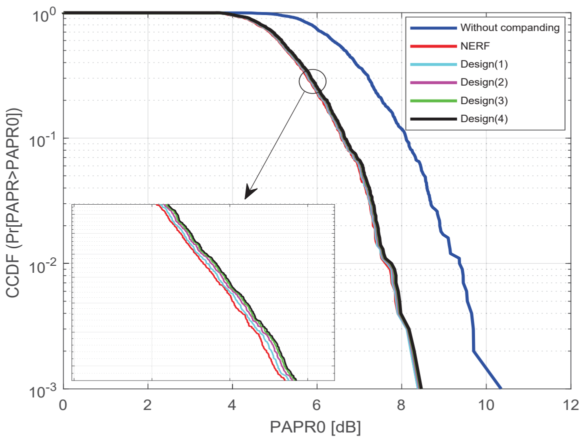

(a)

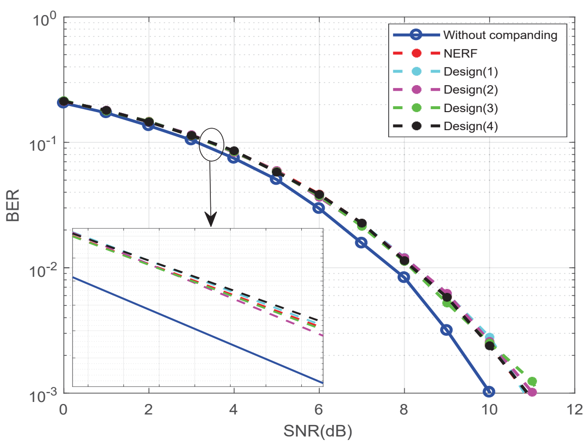

(b)

Fig. (3) Performance comparison of various companding & decompanding techniques with (a): the CCDF vs the PAPR and (b): the BER vs the SNR as the performance metrics of interest.

V. CONCLUSION

Companding the dynamic range of OFDM signals is an efficient technique that reduces the out-of-range clipping-induced non-linear harmonic distortions that frequently occur in practical OFDM systems. In this paper, it is demonstrated that, the companding characteristics of the non-linear error function companding can be realized using the I/O characteristics of the differential tanh-companding MOSFET-based amplifiers. Simulation results confirm that these amplifiers are capable of reducing the PAPR of OFDM signals through the careful control of their key design parameters.

ACKNOWLEDGEMENT

This work by telecommunications regulatory agency of Egypt (NTRA-Egypt).

REFERENCES

[1] T. Hwang, C. Yang, G. Wu, S. Li and G. Y. Li, ”OFDM and Its Wireless Applications: A Survey,” in IEEE Transactions on Vehicular Technology, vol. 58, no. 4, pp. 1673-1694, May 2009.

[2] M. Shehata, and H. Mostafa, ”A Single Wavelength Photonic Network on Chip Design Based on Optical Orthogonal Codes”, IEEE International Symposium on Circuits and Systems (ISCAS 2018), Florence, Italy, pp. 1-4, 2018.

[3] M. Shehata, H. Mostafa, and Y. Ismail, ”On The Theoretical Limits of The Power Efficiency of Photonically Generated IR-UWB Waveforms”, IEEE Journal of Lightwave Technology (JLT), vol. 36, issue 10, pp. 2017 - 2023, 2018

[4] M. Shehata, H. Mostafa, and Y. Ismail, ”Accurate Closed Form Expressions for The Bit Rate-Distance Relationship in IR-UWBoF Systems”, IEEE Communications Letters, vol. 21, issue 10, pp. 2138-2141, 2017.

[5] M. Shehata, H. Mostafa, and Y. Ismail, ”Closed Form Expressions and Bounds for The Signal to Noise Ratio in IR-UWBoF Systems”, IEEE Photonics Technology Letters, vol. 29, issue 6, pp. 507-510, 2017.

[6] M. Shehata, and H. Mostafa, ”Photodetected Power Maximization of Photonically Generated Impulse Radio Ultrawide Band Signals”, IEEE International Symposium on Circuits and Systems (ISCAS 2018), Florence, Italy, pp. 1-4, 2018.

[7] T. Jiang and Y. Wu, ”An Overview: Peak-to-Average Power Ratio Reduction Techniques for OFDM Signals,” in IEEE Transactions on Broadcasting, vol. 54, no. 2, pp. 257-268, June 2008.

[8] I. A. Shaheen, A. Zekry, F. Newagy and R. Ibrahim, ”Modified Square Rooting Companding Technique to Reduced PAPR for FBMC/OQAM,” 2017 Palestinian International Conference on Information and Communication Technology (PICICT), Gaza City, 2017, pp. 66-70.

[9] Tao Jiang, Yang Yang and Yong-Hua Song, ”Exponential companding technique for PAPR reduction in OFDM systems,” in IEEE Transactions on Broadcasting, vol. 51, no. 2, pp. 244-248, June 2005.

[10] Xianbin Wang, T. T. Tjhung and Yiyan Wu, ”On the SER and spectral analyses of A-law companded multicarrier modulation,” in IEEE Transactions on Vehicular Technology, vol. 52, no. 5, pp. 1408-1412, Sept. 2003.

[11] T. Deepa and R. Kumar, ”Performance analysis of μ-law companding & SQRT techniques for M-QAM OFDM systems,” 2013 IEEE International Conference ON Emerging Trends in Computing, Communication and Nanotechnology (ICECCN), Tirunelveli, 2013, pp. 303-307.

[12] P. M. Furth and H. A. Ommani, ”Low-voltage highly-linear transconductor design in subthreshold CMOS,” Proceedings of 40th Midwest Symposium on Circuits and Systems. Dedicated to the Memory of Professor Mac Van Valkenburg, Sacramento, CA, 1997, pp. 156-159 vol.1.

[13] K. S. Ramtej and S. Anuradha, ”New error function companding technique to minimize PAPR in LTE uplink communications,” 2017 Twenty-third National Conference on Communications (NCC), Chennai, 2017, pp. 1-5.

[14] M. A. Khan and R. K. Rao, ”Low-Complexity PAPR Reduction Technique for OFDM Systems Using Biased Subcarriers,” in Canadian Journal of Electrical and Computer Engineering, vol. 39, no. 1, pp. 19-25, winter 2016.

[15] T. Jiang, W. Xiang, P. C. Richardson, D. Qu and G. Zhu, ”On the Nonlinear Companding Transform for Reduction in PAPR of MCM Signals,” in IEEE Transactions on Wireless Communications, vol. 6, no. 6, pp. 2017-2021, June 2007.

[16] Matthias Patzold, and Mattias Paetzold. Mobile fading channels, volume 14. Wiley Online Library, 2002.